Available online at www.sciencedirect.com
SCIENCE DIRECT
Sensors and Actuators B 114 (2006) 239–247
SENSORS AND ACTUATORS B CHEMICAL
www.elsevier.com/locate/snb

Ag/AgCl microelectrodes with improved stability for microfluidics

Brian J. Polk [a,*], Anna Stelzenmuller [a], Geraldine Mijares [a], William MacCrehan [b], Michael Gaitan [a]

[a] *National Institute of Standards and Technology, Semiconductor Electronics Division, 100 Bureau Drive, Stop 8120, Gaithersburg, MD 20899-8120, USA*
[b] *National Institute of Standards and Technology, Analytical Chemistry Division, 100 Bureau Drive, Gaithersburg, MD 20899, USA*

Received 29 November 2004; accepted 23 March 2005
Available online 6 June 2005

Abstract

A method for fabricating Ag/AgCl planar microelectrodes for microfluidic applications is presented. Micro-reference electrodes enable accurate potentiometric measurements with miniaturized chemical sensors, but such electrodes often exhibit very limited lifetimes. Our goal is to construct Ag/AgCl microelectrodes reliably with improved potential stability that are compatible with surface mounted microfluidic channels. Electrodes with geometric surface areas greater than or equal to 100 μm^2 were fabricated individually and in an array format by electroplating silver, greater than 1 μm thickness, onto photolithographically patterned thin-film metal electrodes. The surface of the electroplated silver was chemically oxidized to silver chloride to form Ag/AgCl micro-reference electrodes. Characterization results showed that Ag/AgCl microelectrodes produced by this fabrication method exhibit increased stability compared with many devices previously reported. Electrochemical impedance spectroscopy allowed device specific parameters to be extracted from an equivalent circuit model, and these parameters were used to describe the performance of the microelectrodes in a microfluidic channel. Thus, stable Ag/AgCl microelectrodes, fabricated with a combination of photolithographic techniques and electroplating, were demonstrated to have utility for electrochemical analysis within microfluidic systems.
Published by Elsevier B.V.

Keywords: Micro-reference electrode; Reference electrode; Microelectrode; Ag/AgCl; Microfluidics

1. Introduction

While the theory and practice of reference electrodes for chemical analysis have been established for decades [1–3], there remains much current interest in the practical application of micro-reference electrodes to miniaturized chemical sensors [4–8]. Particularly desirable are fabrication techniques for Ag/AgCl electrodes, which can be compatible with complementary metal-oxide-semiconductor (CMOS) microelectronic circuit fabrication [9–12]. Also of interest are electrodes compatible with microfluidics for separations in lab-on-a-chip systems [7,13,14].

A vexing problem associated with most reported thin-film Ag/AgCl electrodes has been their poor stability. Open circuit potentials are typically observed to be stable for a time period in the range of a few minutes to a few hours [5,8,13,15]. Instability has generally been attributed to dissolution of the very thin layer (few nm) of sparingly soluble AgCl and the subsequently developed mixed potentials at the electrode/solution interface. Silver chloride has a solubility product constant, K_{sp}, of 1.8×10^{-10}, which implies, from a thermodynamic point of view, that about 1.9 mg of AgCl will dissolve in a liter of water at room temperature. On micro-scale terms, a rectangular piece of silver, 100 μm × 100 μm × 1 μm on a side, could be converted entirely to silver chloride and the resulting AgCl could be dissolved in less than 75 μL of water.

A commonly used method of improving stability has been to coat the Ag/AgCl electrode with gel or polymer materials, such as agar or polyurethane [15,16]. The coatings create a diffusion barrier to slow down the rate at which the AgCl dissolves and simultaneously provide a relatively

* Corresponding author. Tel.: +1 301 975 6347; fax: +1 301 948 4081.
E-mail address: brian.polk@nist.gov (B.J. Polk).

0925-4005/$ – see front matter. Published by Elsevier B.V.
doi:10.1016/j.snb.2005.03.121

constant concentration of chloride ion at the Ag/AgCl surface. A buffer layer of Ni between an adhesion layer of Ti and an Ag top coat was recently reported to improve stability [17]. However, the central problem remains; the AgCl coating will dissolve relatively rapidly. In conventional macro-sized electrodes confined to an isolated solution compartment, a small amount of AgCl dissolution from a large wire actually increases potential stability with fluctuating temperatures by saturating the filling solution with AgCl. Such dissolution is fatal to the performance of thin-film electrodes because the very small quantity of AgCl available may entirely dissolve away.

A simple solution to this problem, which does not require polymer coatings is to increase the amount of silver chloride on the microelectrode surface. The typical methods of forming AgCl on Ag include anodization in chloride containing solutions, chemical oxidation and thermal or plasma treatment in chlorine containing atmospheres [11,12,14,15,18–20]. Any of these treatments can produce similar quality AgCl but, applied to a thin layer of silver ($\sim 10^2$ nm thick), they can only result in a thin-film of silver chloride. Therefore, the mass of silver available must be increased. A facile technique to add mass is to electroplate an additional quantity of silver ($\approx 10^3$ nm) onto evaporated thin-film electrodes of either gold or silver. The electroplated silver forms a quasi-bulk phase, which allows for subsequent formation of a much thicker layer of silver chloride. Furthermore, the electroplated silver has a much rougher surface than the evaporated layer, providing a larger electrochemically active surface area in the same geometric footprint of the original microelectrode. Taken together, the large quantity of AgCl and the increased surface area formed by this technique enable stabilization of Ag/AgCl microelectrodes, as demonstrated in this report.

An additional advantage of electroplating silver onto thin-film electrodes is that individual electrodes in an array may be selected for conversion to Ag/AgCl, while leaving others unaltered. To achieve the same type of configurability using either metal evaporation or electroless deposition would require extra mask steps.

Our objective is to create micrometer-sized quasi-reference electrodes and electrode arrays with improved stabilities and lifetimes, which can be used in microfluidic applications. This work discusses practical aspects of the fabrication and characterization of stable Ag/AgCl microelectrodes, both individually and in an array format. The resultant quasi-reference electrodes were characterized with scanning electron microscopy and open circuit potential (OCP) measurements versus an aged commercially available Ag/AgCl macro-reference electrode. The utility of an array of the Ag/AgCl microelectrodes was demonstrated by monitoring potential in a microfluidic channel with applied electric field. Finally, electrochemical impedance spectroscopy was conducted on the microelectrode array in a microfluidic channel, and equivalent circuit modeling helped identify the sources of impedance in the system.

2. Experimental

2.1. Planar electrodes

All electrodes were fabricated by using oxidized silicon (1 0 0) wafers as substrates. Thin-film metal electrodes were patterned onto the substrates by using lift-off metallization techniques [21]. Metals were deposited with thermal evaporation. Cr (≈5 nm) was used as an adhesion layer, and either Ag or Au (≈150 nm) was used as the top layer. In the case of a silver top layer, an intermediate layer of gold (≈50 nm) was used as a barrier between the Cr and the Ag. After lift-off, the entire sample surface was coated with SiO_2. A good passivating insulation was achieved with a thick (≈400 nm) coating of SiO_2 deposited with plasma enhanced chemical vapor deposition (PECVD). Working electrode areas and contact pads were opened by removing the SiO_2 with dilute HF or with reactive ion etching (RIE). A schematic cross-section of the electrode layers and a top–down photograph of the as-fabricated thin-film electrode are shown in Fig. 1.

2.2. Silver electroplating

Surface cleaning was critical to achieving reproducible platings. Electrode samples were cleaned by ultrasonic agitation for 5 min each in isopropyl alcohol, dilute laboratory detergent solution and 1 M HCl (M, mol L^{-1}) with DI water rinse in between. If the electrode showed appreciable current (>10 nA) at zero applied bias in the silver plating bath due to surface contamination, then the cleaning procedure was repeated.

Plating onto clean electrodes was accomplished from 0.3 M $AgNO_3$ in 1 M $NH_{3(aq)}$ by using a three-electrode cell at room temperature. A silver wire served as quasi-reference electrode, and a platinum wire coil served as counter electrode. The following procedure yielded the most repeatable

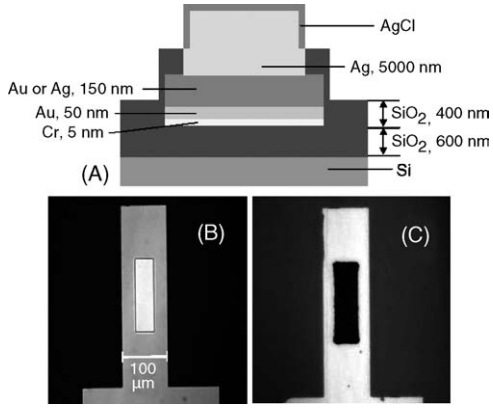

Fig. 1. (A) Schematic diagram of the layer structure of a planar Ag/AgCl microelectrode. Material thicknesses are indicated on the diagram. Drawing not to scale. (B) Top–down photograph of thin-film gold electrode after passivation with PECVD SiO_2 and etching open working area. (C) Top–down photograph of electrode after silver electroplating and oxidizing with ferric chloride.

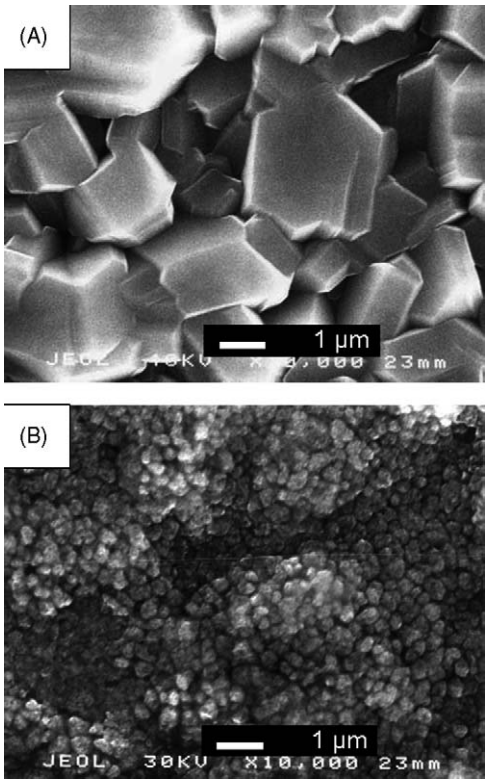

Fig. 2. Scanning electron micrographs of electrode surfaces. (A) Polycrystalline silver as electroplated from silver nitrate in aqueous ammonia solution onto gold at 13 mA/cm^2. (B) Silver chloride particles formed by treating silver surface with 50 mM $FeCl_3$ for 50 s. Note AgCl particles are conformal to the irregular silver surface and have diameters on the order of 100–500 nm.

results among several plating procedures tested. Plating on the planar electrode was performed in two steps. First, an oxidative pre-treatment at +0.95 V was applied for 30 s. The plating solution was agitated after the oxidative pre-treatment to remove any microscopic gas bubbles on the electrode surfaces prior to plating. Then plating was driven at 13 mA/cm^2 for 300 s. On an electrode footprint of 40 μm × 160 μm, the silver layer grew to about 5 μm thick, as estimated with stylus profilometry. The surface was composed of 1 μm to 5 μm diameter crystallites of silver as seen in Fig. 2.

2.3. Silver chloride formation

Both electrochemical anodization in HCl and chemical oxidation with aqueous $FeCl_3$ were investigated as methods to produce the AgCl. Treatment with ferric chloride was much faster to perform and produced a uniform coating of ≈100 nm particles of AgCl, such as those shown in Fig. 2. While the electrode stability was about the same regardless of the oxidation technique, chemically oxidized electrodes tended to have a more ideal Nernstian response in solutions of various chloride ion concentration. The chemical treatment was therefore chosen as the standard oxidation method. A 50 mM solution of $FeCl_3$ was applied to the electroplated silver surface for 50 s at room temperature, followed by rinsing with DI

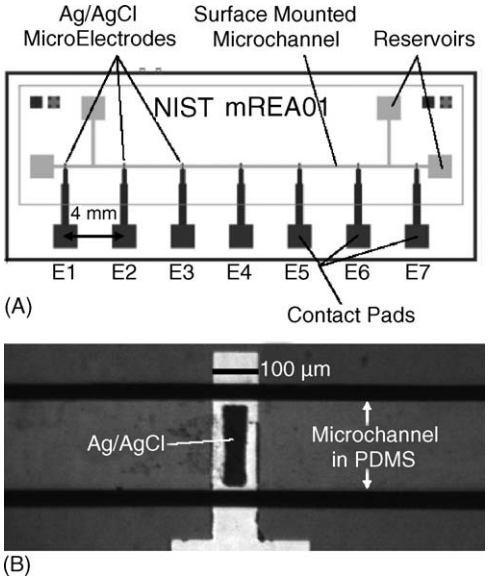

Fig. 3. Ag/AgCl microelectrode array with surface mounted microfluidic channel made from PDMS. (A) Top–down schematic layout of electrode array and microchannel. (B) Top–down photograph of an example Ag/AgCl microelectrode positioned inside of microfluidic channel.

water. This procedure was performed very soon after electroplating to minimize the formation of silver oxide and silver sulfide, which would alter the electrode potentials. The ferric chloride treatment was not specifically optimized, though there was no significant difference noted in electrode stability when different solution concentrations or reaction times were used. Two examples of the silver plated, silver chloride coated electrode are shown in Figs. 1C and 3B.

2.4. Individual microelectrodes

Individual Ag/AgCl microelectrodes with different initial active areas were fabricated as described above. The samples had silver as the top evaporated metal coating. The geometric areas included 1×10^6, 1×10^4 and 1×10^2 μm^2. All electrode sizes were characterized in bulk solutions with different chloride ion concentrations. Samples of 1×10^6 μm^2 area were tested for long-term stability in bulk solution of 1 mM KCl.

2.5. Microelectrode array layout

Electrodes of a 40 μm × 160 μm geometric area were fabricated in an array format. Electrodes were uniformly separated by ca. 4 mm on a planar substrate (see Fig. 3A). Electrode size and spacing were chosen such that the electrodes fit within a surface mounted microfluidic channel. Each electrode sampled a reasonable volume of solution near the middle of the channel width, and the array spanned the majority of the channel length. The top layer of evaporated metal was gold. Silver and silver chloride layers were formed as described above.

Successful silver plating required stringent cleanliness of all apparatus. Because of the very small currents applied to the microelectrodes, any parasitic current caused by contamination had a negative impact on plating quality. All apparatus were therefore cleaned, as appropriate for the given material, with solvent, detergent, or acid washing followed by rinsing with copious amounts of DI water.

2.6. Surface mounted microfluidic channel

The Ag/AgCl microelectrode arrays were used inside of a surface mounted elastomeric microfluidic channel, as shown in Fig. 3B. The channel was molded from poly(dimethyl siloxane) (PDMS) elastomer, cleaned by ultrasonic agitation in isopropyl alcohol, rinsed with DI water and blown dry with N_2, then aligned and sealed over the electrode array [22]. The channel had a trapezoidal cross-section, approximately 45 μm high by 240 μm wide at half height, giving a cross-sectional area of $1.1 \times 10^4\ \mu m^2$. Three molar NaCl solution filled the channel under stagnant flow. Potential steps were applied to the outermost electrodes while potential at in the inner electrodes was simultaneously monitored. In a separate experiment, impedance at each electrode in the array was measured as a function of frequency from 63 kHz to 1 Hz with zero dc bias (versus reference) and 5 mV ac input while using the first electrode as a reference.

3. Results and discussion

3.1. Electrodes without electroplated silver

In order to compare with electroplated electrodes, electrodes with only evaporated silver surfaces treated with either chemical or electrochemical oxidation were also fabricated. However, electrodes of this type did not hold stable open circuit potentials for longer than a few minutes in chloride solutions. It was concluded that a greater quantity of silver and silver chloride was required. The observed instability of electrodes of this type was considered unacceptable for reference electrode performance and the samples were not further characterized.

3.2. Individual microelectrodes

Individual Ag/AgCl electrodes with an evaporated silver surface and subsequent silver electroplating and $FeCl_3$ treatment were studied for long-term potential stability in 1 mM KCl versus an aged commercial Ag/AgCl electrode with 1 mM KCl filling solution and porous glass frit. Data given in Fig. 4 show that electrode samples generally stabilized quickly and held potentials within ±2 mV for at least 1000 min continuously before a large potential discontinuity was detected. At least one of the four replicate samples shown held potential for over 4 days of continuous measurement. Potential values of the replicate samples might differ from each other by approximately 10 mV. The relatively large variation was typically due to a single outlier from a batch. All potentials were somewhat higher than the expected value of near zero volts. This may be attributed to imperfect coverage of electroplated silver, differences in the concentration of Cl^- in the test solution and the macroelectrode filling solution, and the uncertain junction potentials. Stability seemed relatively unaffected by these sources of potential error. The electrode surfaces were examined with scanning electron microscopy after the open circuit potential measurements. The images indicated that the AgCl particles were absent from the Ag surface, which supported the view that loss of the AgCl results in poor electrode stability.

The single electrode samples were also tested for Nernstian response to chloride ion activity. Activity of the solution of known salt concentration was estimated from Debye–Hückel theory. In the concentration range from 100 to 1 mM, the electrodes of the $1 \times 10^6\ \mu m^2$ geometric area responded with a mean slope of 51.5 mV/decade with good repeatability between electrode samples of about 1% relative error. Electrodes of smaller geometric area were similarly tested. Electrode geometric areas of $1 \times 10^4\ \mu m^2$ gave a mean

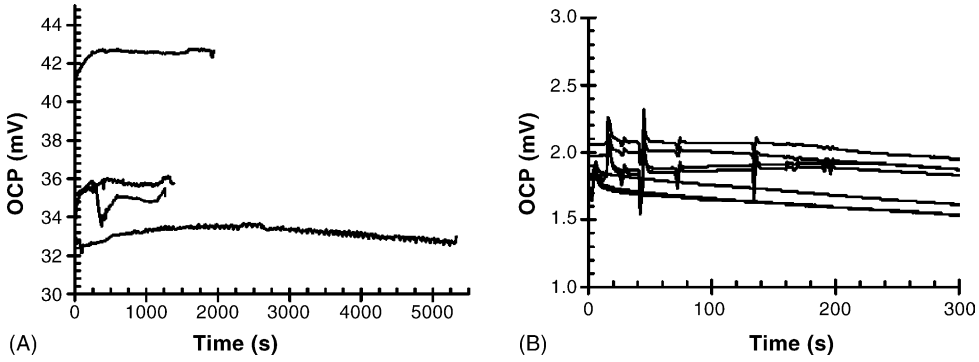

Fig. 4. Open circuit potentials of Ag/AgCl microelectrodes in bulk solution vs. an aged Ag/AgCl macro-reference electrode obtained commercially. (A) Four replicate samples of microelectrodes with geometric areas of $1 \times 10^6\ \mu m^2$ in 1 mM KCl over a period of days. (B) Array of seven microelectrodes with geometric areas of $6.4 \times 10^3\ \mu m^2$, initial potentials in 3 M NaCl.

slope of 49.2 mV/decade, and 1×10^2 μm^2 gave a slope of 52.1 mV/decade but with higher relative errors of 6% and 14%, respectively.

The original electrode geometric area was seen to have some effect on the long-term stability tests. The larger area electrodes tended to stay stable for a longer time, again attributable to the relative amount of Ag/AgCl available. Furthermore, the smallest electrodes tended to be slightly more difficult to plate uniformly with silver. In the larger electrodes, silver grains formed at many nucleation sites and tended to grow together during the plating process, leading to a uniform surface coverage. At the smaller electrodes, a single nucleation site may form a silver crystallite with a surface area close to that of the original surface. The crystallite would then dominate the subsequent plating because of radial diffusion profiles and concentrated electric fields, leaving much of the original surface un-coated. Subsequent dissolution of the thin AgCl layer on the unplated surfaces would expose the underlying metals to the electrolyte after which mixed potentials would be formed and the electrode would become unstable. Organic additives, known as levelers, might be added to the plating bath to promote better coverage of the smaller electrodes.

3.3. Microelectrode array

A high quality coverage (i.e., plating covered all of the electrode surface, dense packing of crystallites, and very little overgrowth) of electroplated silver on all electrodes in the array format could be obtained with good repeatability only with stringent cleanliness. Even with very clean devices and apparatus, inconsistent plating quality on electrodes in the same array was occasionally observed. It was found that a qualitative assessment of the quality of the silver plating by visual inspection of the electrode surface strongly correlated with the probability that the electrode would give a stable potential near the ideal value.

Microelectrode stability in the array was measured in a bulk container of 3 M NaCl, saturated with AgCl versus an aged commercial Ag/AgCl macro-electrode with porous glass frit with 3 M NaCl filling solution. Fig. 4B gives an example of the initial potential compared with the macro-electrode for an array of Ag/AgCl electrodes with high quality silver coverage. All values in the data set shown clustered less than 1 mV with respect to each other. However, it was not unusual for a single electrode in an array to measure outside the main cluster. Drift was estimated to be less than 1 $\mu V\,s^{-1}$. All the data in this set were measured only 2 mV off the ideal value of zero. Such a small error may be attributed to uncertain junction potentials or slight differences in the chloride activity in the test solution and the macro-reference filling solution.

Electrode stability was noted to be approximately equivalent, regardless of chloride ion concentration, though obviously the magnitude of the potential shifted. A 3 M solution was chosen for this work because it closely matched the macro-reference electrode filling solution provided by the commercial manufacturer. Potential stability in other buffers was generally found to be similar, including the cell culture media, DMEM/F12 [23], though the basic pH caused an error in the expected positive potential shift from 81 to 65 mV.

The last evaporated layer in the array was gold while, in the single electrodes, it was silver. However, there was no observed difference in electrode stability based on the type of evaporated metal layer. This was because the electroplated silver completely covered the evaporated layer and was present in much greater quantity. The electrolyte solution therefore only contacted the plated Ag/AgCl. There may have been a small contact resistance between the dissimilar metals, but the data indicated that the metal/metal interface could be treated as an equi-potential surface, and the possible contact resistance was therefore ignored in the subsequent analysis.

3.4. Noise in bulk solutions

A feature noted in this data was the induced noise, which appears periodically during the open circuit potential measurement. This noise was attributed to environmental disturbances (e.g., vibrations, drafts, etc. creating stray electric fields) disrupting the stability of the electrode/solution interface and was more pronounced for electrodes of smaller geometric area. The potentials of smaller electrodes were disturbed to a relatively greater extent because of the smaller surface area in contact with solution. This observation leads to the recommendation that very small electrodes be shielded in a Faraday cage during measurement to reduce the noise influence when high precision is required. Further, a low-pass filter could also be incorporated in the measurement circuit. Alternatively, the electrodes might be used as sensitive detectors of stray electric fields.

3.5. Use of Ag/AgCl electrodes to observe potentials in a microfluidic channel

The application of small, planar micro-reference electrodes to monitor potential inside of a microfluidic channel under the influence of applied electric field was demonstrated with the Ag/AgCl electrode array (see Fig. 3 for array and microchannel layout). Potential steps of ± 20 mV were applied to E1 with respect to E7 (abbreviated $E1_{E7}$). Potential was simultaneously monitored at E3, E5 and E6 with respect to E2 (abbreviated $E3_{E2}$, $E5_{E2}$, $E6_{E2}$) with a near zero current in the measurement circuit. The input potential steps, measured E1 to E7 current, and measured potentials of $E3_{E2}$, $E5_{E2}$ and $E6_{E2}$ are given in Fig. 5. $E3_{E2}$, $E5_{E2}$ and $E6_{E2}$ were normalized to zero initial potential and then offset for clarity. Current between E1 and E7 followed an expected Cottrell-like decay with time. Potentials measured in the channel closely followed the changes in current, and the sign of the potentials with respect to E2 also followed, as expected.

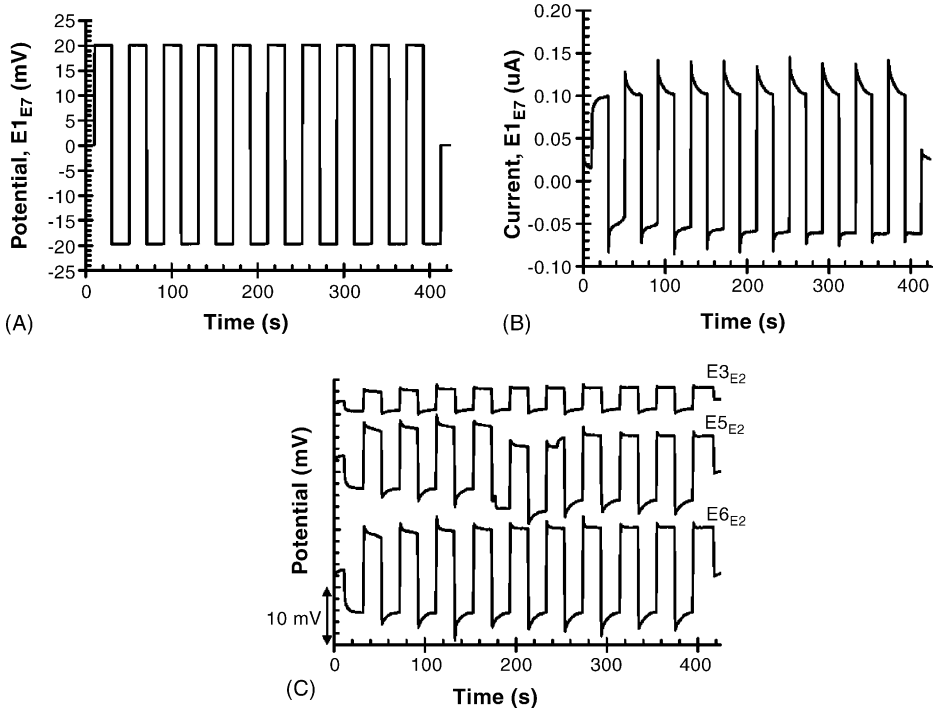

Fig. 5. Measured applied voltage, current and potentials between electrodes in a microchannel. The microchannel was filled with 3 M NaCl. (A) ±20 mV potential steps applied between E1 and E7 to induce the electric field. (B) Measured current between E1 and E7 during potential steps. (C) Potential measured at E3, E5 and E6 all vs. E2 during potential steps at $E1_{E7}$. Data were offset for clarity.

When the quasi-steady potentials (Fig. 5C) were divided by the corresponding current in the channel (Fig. 5B), an estimate of the resistance of the channel could be calculated. The average resistance over several external potential pulses was found to be 23.2, 69.9 and 91.1 kΩ for $E3_{E2}$ (one electrode spacing), $E5_{E2}$ (three electrode spacing) and $E6_{E2}$ (four electrode spacing), respectively. Because the electrodes were evenly spaced, the resistance between any arbitrary pair of electrodes should be unit multiples of the resistance between adjacent electrodes. This was experimentally confirmed. The resistance between E5 and E2 (three electrodes spacing) was found to be 3.01 times the resistance between E3 and E2 (adjacent electrodes). The resistance between E6 and E2 (four electrodes spacing) was found to be 3.93 times the resistance between E3 and E2. All three resistances were averaged to give an estimate of the channel resistance between two adjacent electrodes, found to be 23.1 kΩ, or on a per unit length basis, 5.76 kΩ/mm. This value was reasonable given the channel dimensions (area = 1.1×10^{-4} cm^2 and length = 0.4 cm) and the estimated conductivity of 3 M NaCl solution (σ in the order of 0.2 S/cm), giving an expected resistance of approximately 18 kΩ between two electrodes.

When the resistance of the channel was estimated from the quasi-steady state current (Fig. 5B) and the known potential input, $E1_{E7}$ (Fig. 5A), the resistance between the electrodes was found to be 255 kΩ total or 42.5 kΩ between two adjacent electrodes (10.6 kΩ/mm), almost twice that measured inside the channel. The source of the discrepancy was clarified by tracing the current path. When current was forced through E1 and E7, it passed not only through the channel, but through the electrode double layer as well. The resistance of the double layer was of similar magnitude to the resistance of the channel itself, leading to the larger total resistance value. When potential was measured on the inner electrodes, the high input impedance meters utilized ensured that almost no current passed through the electrode interface. Corresponding measured potential differences therefore yielded a better estimate of the channel resistance, separate from the resistance of the interface. Subtracting the channel resistance from the resistance of the (channel + electrode) gave an estimate of the resistance of the electrode itself and in this case yielded a value of approximately 10 kΩ per electrode.

3.6. Noise in microchannel

Noise similar to that observed in bulk solutions was also observed when the electrodes were placed inside the microchannel. The small solution volume seemed to exacerbate the problem, leading to deviations from median potentials of greater magnitude than those seen in the bulk solutions. Again the noise was attributed to environmental factors and reinforced the need for shielding and noise filtering. Luckily, the noise did not seem to affect the baseline OCP, and the electrode would typically return to a quiet potential a few seconds after the disturbance. Thus, monitoring step changes in potential was still reliable.

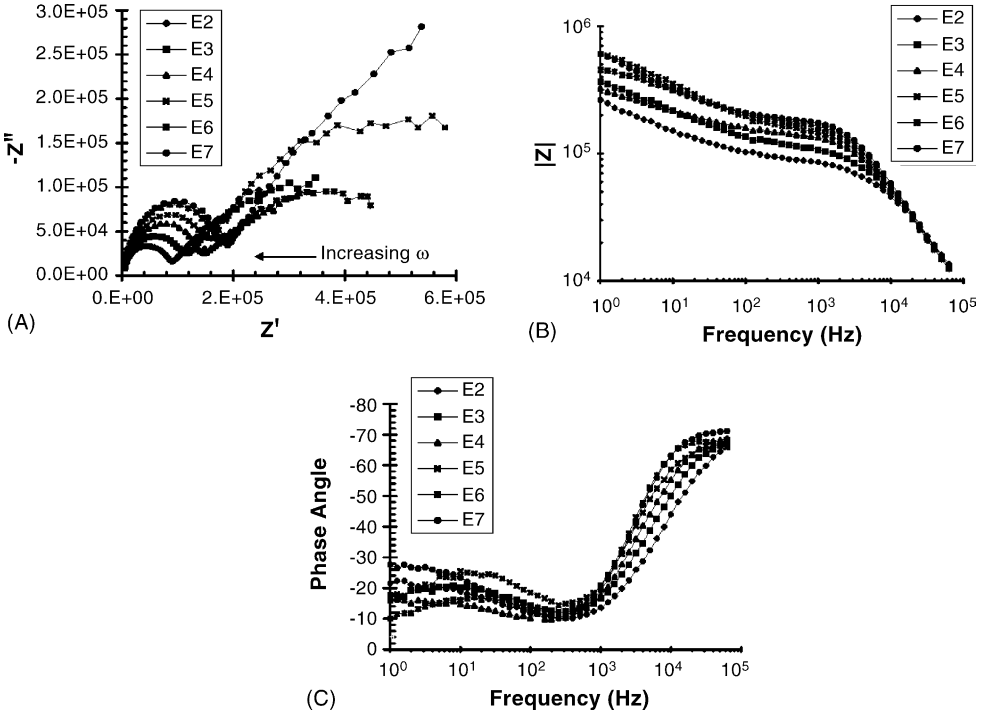

Fig. 6. Impedance analysis of Ag/AgCl microelectrode array inside of microfluidic channel filled with 3 M NaCl. Impedance measured at E2, E3, E4, E5, E6 and E7 with respect to E1. Zero dc bias vs. E1 with 5 mV ac input signal. Connector lines between data points as a visual aid. (A) Bodé plot. Each point gives the real and imaginary components of impedance at a single frequency. Frequency increases from right to left, as indicated on the plot. (B) Absolute magnitude of impedance as a function of frequency. (C) Phase angle as a function of frequency.

3.7. Electrochemical impedance spectroscopy in a microfluidic channel

Considering the importance of impedance in electrochemical measurements, electrochemical impedance spectroscopy was carried out inside of a microfluidic channel with an array of matched Ag/AgCl microelectrodes; the resulting data are given in Fig. 6. The Bodé plot indicated a clear trend with electrode separation in the microchannel. Equivalent circuit modeling helped deconvolute the impedance contribution from each interface in the system. The model used to fit the experimental data is given in Table 1. It consisted of four components in series: one constant R, two RC parallel circuits, and one R in parallel with a constant phase element (CPE). The unconstrained fitting parameters are listed in Table 1 [24]. Goodness of fit was indicated with Chi^2, the square of the standard deviation between the raw data and the calculated curve, and with Sum Sq, the weighted sum of squares, which

Table 1
Unconstrained fit parameters for the impedance model, as indicated

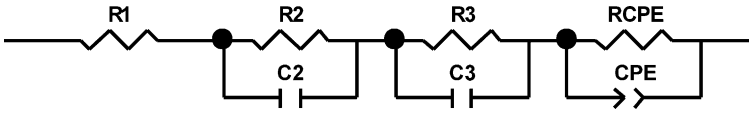

	Electrode label					
	E2	E3	E4	E5	E6	E7
R_1 (kΩ)	0.62	1.55	1.75	1.96	1.84	1.48
R_2 (kΩ)	46.8	64.8	94.6	118.6	144.9	154.8
C_2 ($\times 10^{-10}$ F)	7.28	6.65	5.47	4.09	3.44	3.2
R_3 (kΩ)	24.64	27.91	28.24	12.68	5.52	8.17
C_3 ($\times 10^{-10}$ F)	3.39	3.89	4.45	5.58	8.46	9.05
CPE-T ($\times 10^{-10}$ F)	2.19	0.81	1.28	0.29	0.39	0.64
CPE-P	0.393	0.488	0.451	0.582	0.55	0.514
R_{CPE} (kΩ)	1384.3	524.2	447.7	703.6	411.5	2202.5
Chi^2	0.000414	0.000412	0.000429	0.000511	0.000365	0.000238
Sum Sq	0.0356	0.0354	0.0373	0.0439	0.0314	0.0205

is proportional to the average percentage error between the raw data and the calculated values. The very small values of both Chi^2 and Sum Sq indicated that the model was a very good fit to the data.

A more common impedance model of only one parallel *RC* in series with another *R* could not be used in this instance for two reasons. First, the reference electrode and the working electrode were of similar area. This implies a similar current density at each electrode, and therefore the contribution of the reference electrode to the impedance spectra could not be ignored. Second, the solution was confined to a microfluidic channel, which implied significant impedance due to the small cross-sectional area despite the low resistivity of the solution.

The constant phase element was fit to the data with a nearly constant "non-ideality parameter" (CPE-P) of about 0.5, indicating a slow diffusion process and a Warburg impedance. Capacitance varied from 10^{-7} to 10^{-6} F. The corresponding resistance, R_{CPE}, was quite high, about 0.5 MΩ or greater. From this information, the CPE circuit component might be attributed to the movement of charge through the solid AgCl layer. In such a case, the mobile charge was likely silver ion [25,26]. The possibility exists that the CPE component represents a capacitive coupling and mobile charges in the silicon oxide layers. However, this interpretation was ruled out because the fitting parameters did not scale with electrode separation.

R_2C_2 yielded a nearly linear correlation between resistance and electrode separation within the microchannel. The R_2 value between E2 and E1 was modeled to be 46.8 kΩ, and the average difference between any two adjacent electrodes, E2 through E7, was calculated to be 21.6 kΩ. These values are in close agreement with the electrode resistance values found during the potential step experiments. Therefore, R_2 was taken to be the resistance felt by a test charge traversing the reference electrode double layer, the microchannel, and then the working electrode double layer.

The component R_3C_3 was attributed to the contribution of the electrode double layer to the signal. Because the reference and working electrodes were of similar surface area and therefore current density, the value of R_3 for closely spaced electrodes was calculated around 25 kΩ. Past a certain separation distance, R_3 dropped to around 10 kΩ, which would be the value expected for only one electrode. It was speculated that the resistance of the channel was much greater than the double layer past a certain critical distance and only the working electrode was measured. These resistances are in agreement with the estimated electrode resistance given in the potential step experiments. Notice that as C_2 decreases with electrode separation, C_3 increases with roughly the same total capacitance. This would be expected for electrode interfaces with similar surface areas and compositions.

R_1 seems related to the small dc bias applied to the working electrode in order to hold it at 0 V versus the reference electrode. The current estimated from the initial OCP between the working and reference electrode and the value of R_1 gives microampere currents, which generally decrease with increasing electrode separation. The experimental condition of zero bias versus the reference electrode actually leads to an applied bias versus the open circuit potentials, inducing a small and relatively constant current. R_1 is in fact an indicator of this relationship.

It would be incorrect to infer electrode impedance directly as a function of active area in these devices because the actual surface area available was uncertain. Resistance should scale inversely with area. An estimate of the product of resistance and area has a lower bound of $6.4 \times 10^7\ \Omega\ \mu m^2$ based on the surface area of the bare (not electroplated) surface. Actual resistance times area should be higher than this value because of the increased surface area of the rough surface of the electroplated Ag and AgCl.

From the above discussion, it seemed reasonable to speculate that impedance spectroscopy and equivalent circuit modeling may be a useful tool for analysis of microfluidic systems in general. By using this analysis, the properties of fluids in the microchannel were separated from the properties of the electrodes themselves. Importantly, confidence in such an analysis was greatly improved when measurements were made with stable micro-reference electrodes.

4. Conclusions

A reliable method for fabricating stable, planar Ag/AgCl electrodes on a micrometer scale was developed. Thin-film electrodes were coated with electroplated silver metal and the surface converted to silver chloride by chemical oxidation. The resulting surfaces were characterized with scanning electron microscopy and were found to have a larger surface area when compared with the geometric footprint of the electrode. The relatively large amount of silver chloride thus made available led to a greatly increased potential stability; in some cases electrodes were found to be stable over 4 days. Microelectrodes of various geometric areas subjected to similar surface treatments were shown to respond in a nearly Nernstian fashion to solutions of different chloride ion activity.

Ag/AgCl microelectrodes were fabricated in an array format as part of this study. Complete arrays of electrodes were shown to have stable, repeatable potentials in high concentration chloride solutions. The utility of the electrode array in a microfluidic system was demonstrated. Potential inside a microchannel during application of an electric field was measured. Electrochemical impedance spectroscopy inside of the microchannel was carried out, and results closely matched those observed in the potential step experiments. Equivalent circuit modeling of the system was shown to deconvolute the contributions of the channel impedance independent of the electrode impedance.

While environmental noise clearly needs to be addressed further, an array of stable Ag/AgCl microelectrodes may find additional applications in other microfluidic systems.

An example might be electrochemical detection and characterization of DNA or protein separations. Future work will focus on integrating the microelectrode array with CMOS electronics, such as an operational amplifier. Constructing an electrode array with an amplifier and other circuitry integrated on the same chip may lead to enhanced signal detection by decreasing loading and also reduce the effects of environmental disturbance.

Acknowledgments

This work was supported in part by the NIST Single Molecule Manipulation and Measurement Competence Program. B. J. P. acknowledges the National Research Council/NIST post-doctoral fellowship. A. S. of Southern Methodist University, Dallas, TX conducted portions of this research as part of a Summer Undergraduate Research Fellowship (SURF), sponsored by the National Science Foundation under grant number 0139217.

Portions of this work were performed at the NIST Semiconductor Electronics Division Microfabrication Process Facility managed by R. Hajdaj.

References

[1] G.J. Janz, Silver–silver halide electrodes, in: D.J.G. Ives, G.J. Janz (Eds.), Reference Electrodes, Academic Press, New York, 1961.
[2] R.G. Bates, V.E. Bower, Standard potential of the silver–silver-chloride electrode from 0 °C to 95 °C and the thermodynamic properties of dilute hydrochloric acid solutions, Original citation: J. Res. Natl. Bur. Stand., 53 (1954) 283–290, reprinted citation: J. Res. Natl. Stand. Technol., 106 (2001) 471–478.
[3] J. Janata, Principles of Chemical Sensors, Plenum Press, New York, 1989, pp. 81–239.
[4] E. Bakker, M. Telting-Diaz, Electrochemical sensors, Anal. Chem. 74 (2002) 2781–2800.
[5] T. Matsumoto, A. Ohashi, N. Ito, Development of a micro-planar Ag/AgCl quasi-reference electrode with long-term stability for an amperometric glucose sensor, Anal. Chim. Acta 462 (2002) 253–259.
[6] G. Jobst, I. Moser, M. Varahram, P. Svasek, E. Aschauer, Z. Trajanoski, P. Wach, P. Kotanko, F. Skrabal, G. Urban, Thin-film microbiosensors for glucose–lactate monitoring, Anal. Chem. 68 (1996) 3173–3179.
[7] O.C. Keller, J. Buffle, Voltammetric and reference microelectrodes with integrated microchannels for flow through microvoltammetry. 1. The microcell, Anal. Chem. 72 (2000) 936–942.
[8] H. Suzuki, T. Hirakawa, S. Sasaki, I. Karube, An integrated three-electrode system with a micromachined liquid-junction Ag/AgCl reference electrode, Anal. Chim. Acta 387 (1999) 103–112.
[9] M. Morita, M.L. Longmire, R.W. Murray, Solid-state voltammetry in a three electrode electrochemical cell-on-a-chip with a microlithographically defined microelectrode, Anal. Chem. 60 (1988) 2770–2775.
[10] J.C. Ball, D.L. Scott, J.K. Lumpp, S. Daunert, J. Wang, L.G. Bachas, Electrochemistry in nanovials fabricated by combining screen printing and laser micromachining, Anal. Chem. 72 (2000) 497–501.
[11] H. Suzuki, H. Shiroishi, S. Sasaki, I. Karube, Microfabricated liquid junction Ag/AgCl reference electrode and its application to a one-chip potentiometric sensor, Anal. Chem. 71 (1999) 5069–5075.
[12] C.D. Bratten, P.H. Cobbold, J.M. Cooper, Micromachining sensors for electrochemical measurement in subnanoliter volumes, Anal. Chem. 69 (1997) 253–258.
[13] J. Wang, R. Polsky, B. Tian, M.P. Chatrathi, Voltammetry on microfluidic chip platforms, Anal. Chem. 72 (2000) 5285–5289.
[14] R.P. Baldwin, T.J. Roussel Jr., M.M. Crain, V. Bathlagunda, D.J. Jackson, J. Gullapalli, J.A. Conklin, R. Pai, J.F. Naber, K.M. Walsh, R.S. Keynton, Fully integrated on-chip electrochemical detection for capillary electrophoresis in a microfabricated device, Anal. Chem. 74 (2002) 3690–3697.
[15] J.S. Lee, S.D. Lee, G. Cui, J.J. Lee, J.H. Shin, G.S. Cha, H. Nam, Hydrophilic polyurethane coated silver/silver chloride electrode for the determination of chloride in blood, Electroanalysis 11 (1999) 260–267.
[16] I.Y. Huang, R.S. Huang, L.H. Lo, Improvement of integrated Ag/AgCl thin-film electrodes by KCl-gel coating for ISFET applications, Sens. Actuators B, Chem. 94 (2003) 53–64.
[17] H.R. Kim, Y.D. Kim, K.I. Kim, J.H. Shim, H. Nam, B.K. Kang, Enchancement of physical and chemical properties of thin film Ag/AgCl reference electrode using a Ni buffer layer, Sens. Actuators, B, Chem. 97 (2004) 348–354.
[18] A. Arevalo, R.M. Souto, M.C. Arevalo, Preparation and reproducibility of a thermal silver–silver chloride electrode, J. Appl. Electrochem. 15 (1985) 727–735.
[19] S.I. Park, S.B. Jun, S. Park, H.C. Kim, S.J. Kim, Application of a new Cl-plasma-treated Ag/AgCl reference electrode to micromachined glucose sensor, IEEE Sens. J. 3 (2003) 267–273.
[20] X. Jin, J. Lu, P. Liu, H. Tong, The electrochemical formation and reduction of a thick AgCl deposition layer on a silver substrate, J. Electroanal. Chem. 542 (2003) 85–96.
[21] S.A. Campell, The Science and Engineering of Microelectronic Fabrication, Oxford University Press, New York, 1996, pp. 274–275.
[22] J.C. McDonald, D.C. Duffy, J.R. Anderson, D.T. Chiu, H.K. Wu, O.J.A. Schueller, G.M. Whitesides, Fabrication of microfluidic systems in poly(dimethylsiloxane), Electrophoresis 21 (2000) 27–40.
[23] Dulbecco's Modification of Eagle's Medium/Ham's F-12. Concentration of Cl^- approximately 0.125 M.
[24] Model fitting performed with ZView software, Version 2.6, Scribner Associates Inc. 2002, the software package is identified in this report to adequately specify the experimental procedure. Such identification does not imply recommendation or endorsement by the National Institute of Standards and Technology nor does it imply that the software is necessarily the best available for the purpose.
[25] R.K. Rhodes, R.P. Buck, Impedance characterization of anodized silver–silver chloride electrodes, Anal. Chim. Acta 113 (1980) 55–66.
[26] J. Jamnik, J. Maier, S. Pejovnik, Interfacial impedance of the boundary Ag/AgCl and its investigations by a novel method, Solid State Ionics 80 (1995) 19–26.